Ventricular remodeling.
from the cath table to the aquarium

Daniel R. Wagner

Outcome

2002: Stenting of RCA
Diabetes, atrial fibrillation, depression, small CVA, ICD

	2002	2003	2004	2005	2006	2007	2008	2009	2010	2011
NYHA	4	2	2	2	2	2	3	3	3	3
weight	75	76	76	84	85	85	82	80	76	75
EF	18%	35%	23%	18%	20%	25%	25%	25%	24%	18%
Crea	1.3	1.5	1.9	1.8	2.2	2.7	2.6	2.8	2.7	2.8
Hb	nl	nl	nl	nl	12.2	12.5	12.3	11.6	11.4	11.9
Pro-BNP			12,906					12,447	32,770	22,014
BNP				402	533	694	1700			
TNT	2.0	nl	nl	nl	nl	nl	0.04	0.05	0.05	0.05

P4
Personalized Medicine

- Personalized
- Predictive
- Preventive
- Participatory

LV Volume changes in 400 patients from the Leicester Acute MI study

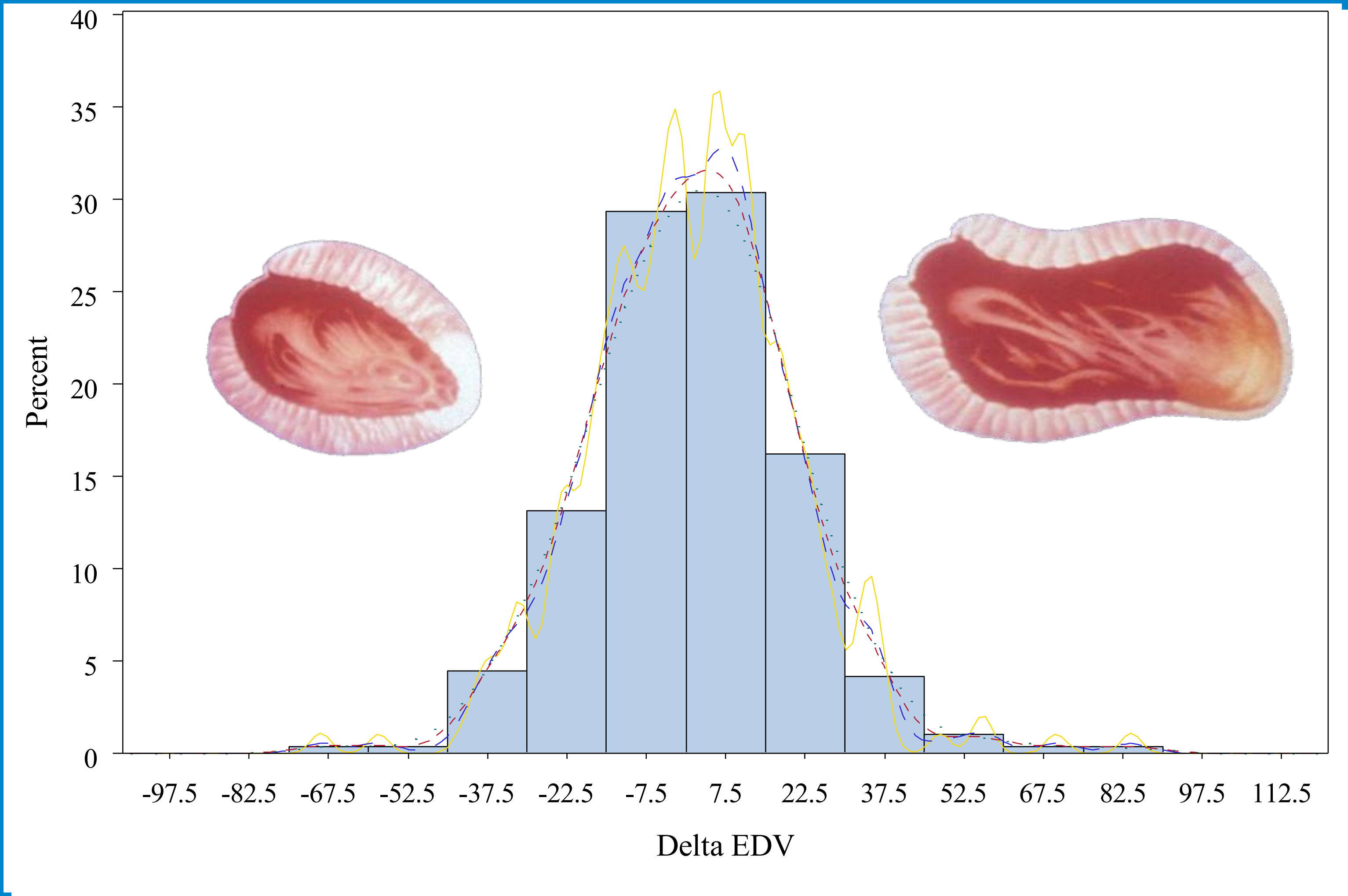

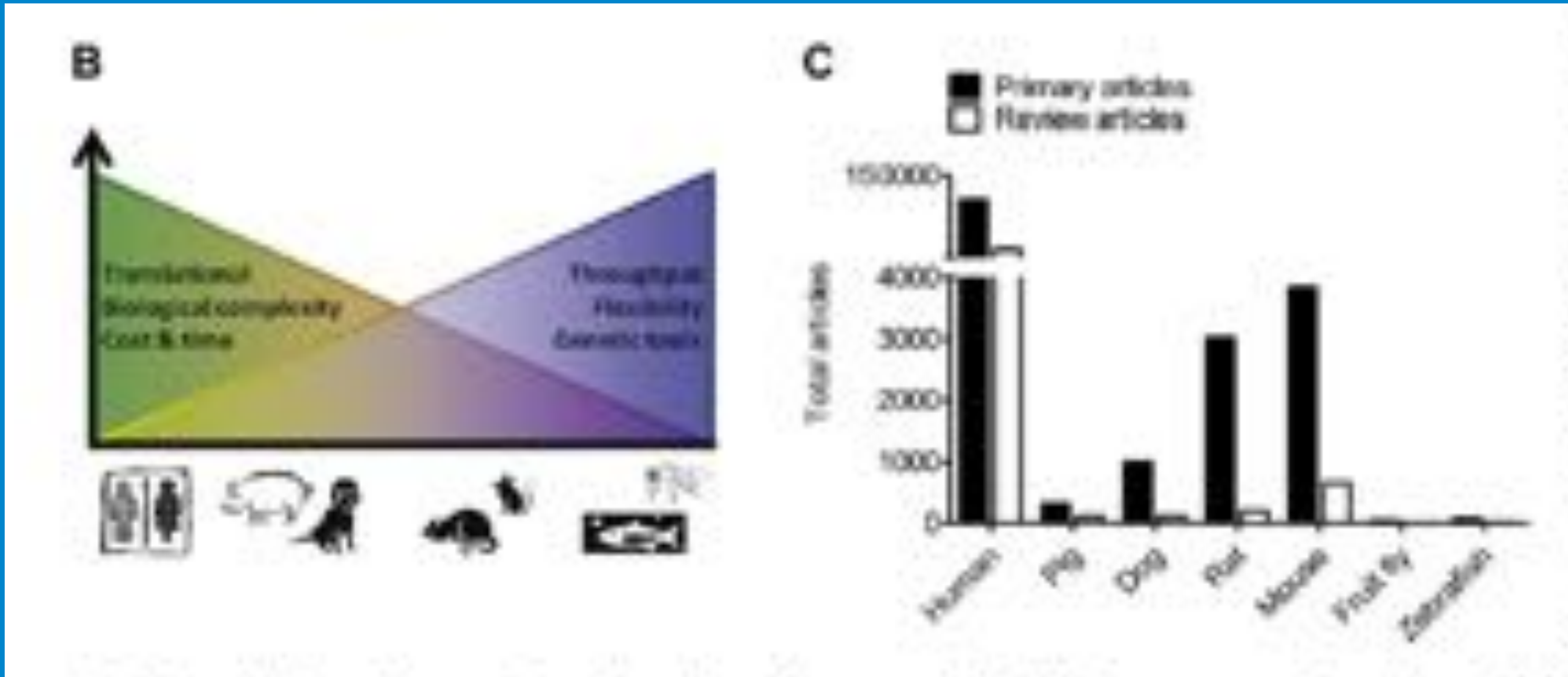

Proteomics Clin Appl 2014

LUCKY

MMP-9

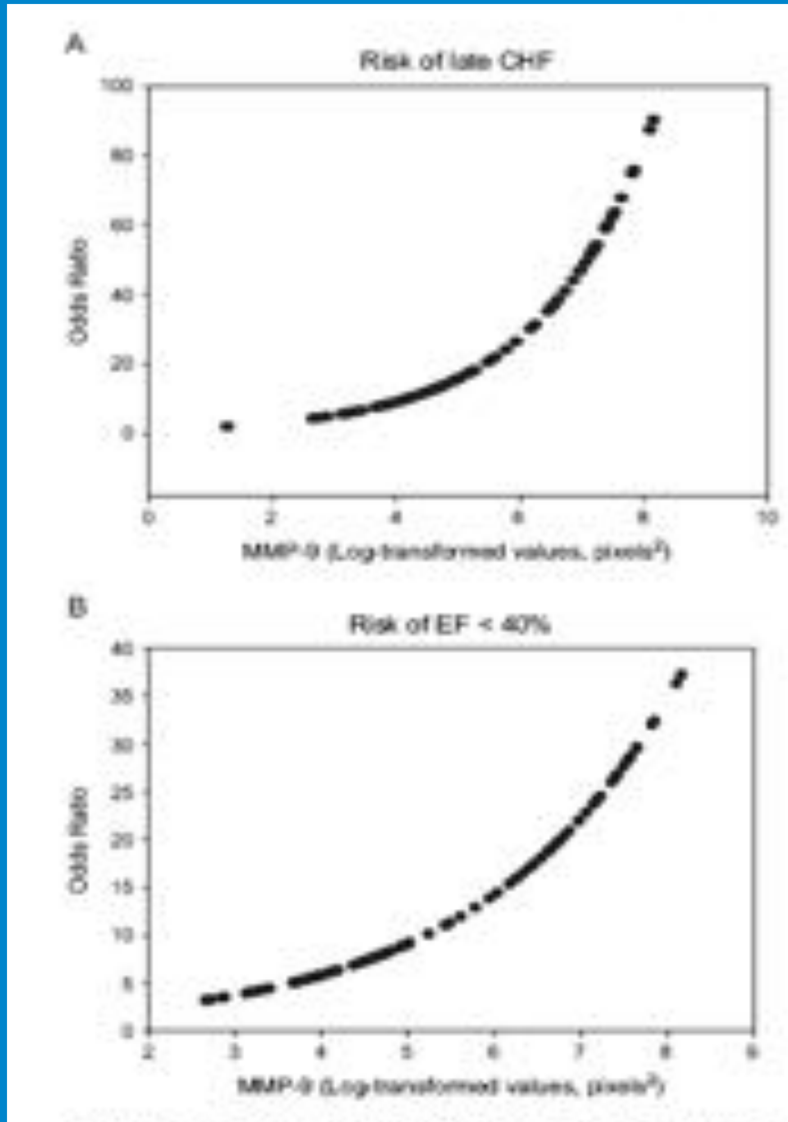

J Card Fail 2006;12:66

MMP-9 gene

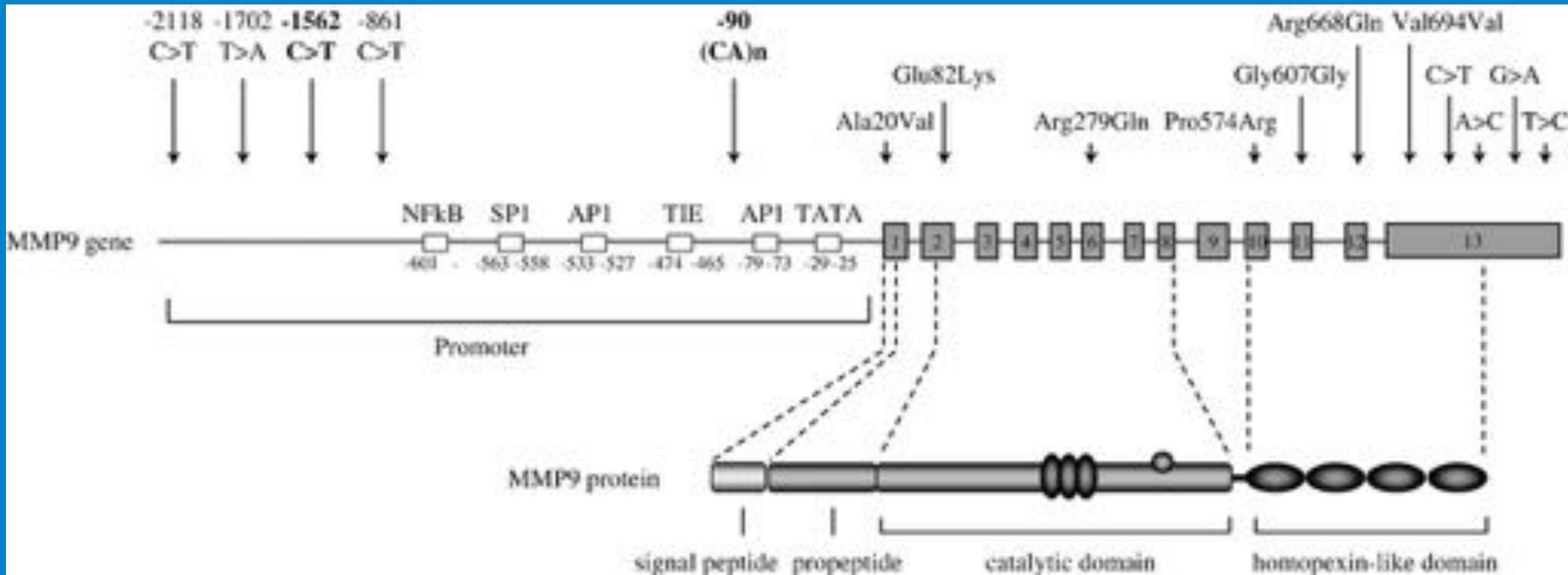
-2118 C>T
-1702 T>A
-1562 C>T
-861 C>T
-90 (CA)n
Ala20Val
Glu82Lys
Arg279Gln
Pro574Arg
Gly607Gly
Arg668Gln
Val694Val
C>T
G>A
A>C
T>C
MMP9 gene
NFkB
SP1
AP1
TIE
AP1
TATA
Promoter
MMP9 protein
signal peptide
propeptide
catalytic domain
homopexin-like domain

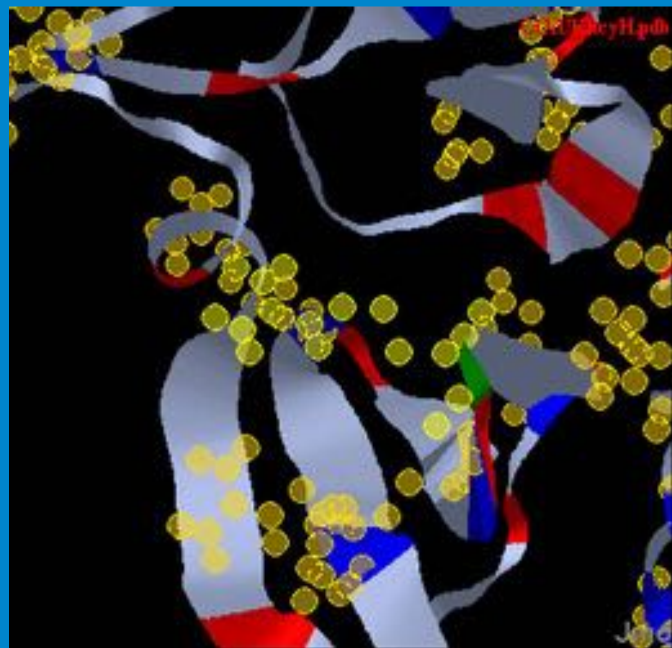

Results of the Genetic Sub-study of the Surgical Treatment for Ischemic Heart Failure (STICH) Trials

24 Genetic Markers	Wild Type (Patients/Events)	Variant (Patients/Events)	Hazard Ratio	95% CI	P-value
1) Beta 1 adrenergic receptor-389c/g	296 / 110	236 / 104	1.06	(0.81, 1.39)	0.686
2) Beta 1 adrenergic receptor-s49g	417 / 172	115 / 43	1.01	(0.72, 1.43)	0.933
3) Beta 2 adrenergic receptor-164	518 / 209	13 / 5	1.35	(0.55, 3.31)	0.506
4) Beta 2 adrenergic receptor-arg16gly	82 / 37	460 / 178	0.86	(0.60, 1.22)	0.390
5) Beta 2 adrenergic receptor-gln27glu	188 / 82	346 / 133	0.81	(0.62, 1.07)	0.147
6) Angiotensin converting enzyme-i/d	128 / 53	404 / 162	0.81	(0.59, 1.11)	0.192
7) Adenosine 1 receptor A1-717T/G	257 / 92	273 / 121	1.15	(0.88, 1.51)	0.310
8) Adenosine 1 receptor A1-Del36	517 / 209	14 / 5	0.74	(0.30, 1.82)	0.518
9) Adenosine 1 receptor A1-1689-C/A	485 / 199	45 / 14	0.67	(0.39, 1.16)	0.156
10) Adenosine 1 receptor A1-2206 Tdel	491 / 200	38 / 12	0.61	(0.34, 1.10)	0.101
11) Angiotensin-M235T	140 / 54	383 / 161	1.31	(0.96, 1.79)	0.091
12) Adenosine monophosphate deaminase 1	390 / 152	142 / 63	1.10	(0.82, 1.48)	0.519
13) Cyp11b2 (aldosterone synthase gene)-344c/t c=1	107 / 46	425 / 169	0.90	(0.65, 1.25)	0.527
14) Matrix metalloproteinase type 9-7254	374 / 154	158 / 61	1.02	(0.76, 1.38)	0.898
15) Matrix metalloproteinase type 9-7279	394 / 159	138 / 56	1.10	(0.81, 1.50)	0.528
16) Matrix metalloproteinase type 9-1562	394 / 155	138 / 60	1.13	(0.84, 1.53)	0.423
17) Matrix metalloproteinase type 9-e6	137 / 49	395 / 166	1.02	(0.74, 1.40)	0.924
18) Matrix metalloproteinase type 9-e13+6c/t	115 / 48	417 / 167	0.84	(0.61, 1.16)	0.287
19) Nitric oxide synthase type 3-4a/4b	365 / 142	166 / 72	1.08	(0.81, 1.44)	0.591
20) Nitric oxide synthase type 3-786	74 / 35	458 / 180	0.87	(0.60, 1.25)	0.454
21) Nitric oxide synthase type 3-894	262 / 101	270 / 114	1.04	(0.79, 1.36)	0.798
22) Monocyte chemoattractive protein-2136a/t	360 / 142	172 / 73	1.17	(0.88, 1.56)	0.271
23) Monocyte chemoattractive protein-2578a/g	267 / 112	266 / 103	0.93	(0.71, 1.22)	0.623
24) Tumor necrosis factor-g308a	16 / 6	517 / 208	1.46	(0.62, 3.41)	0.385

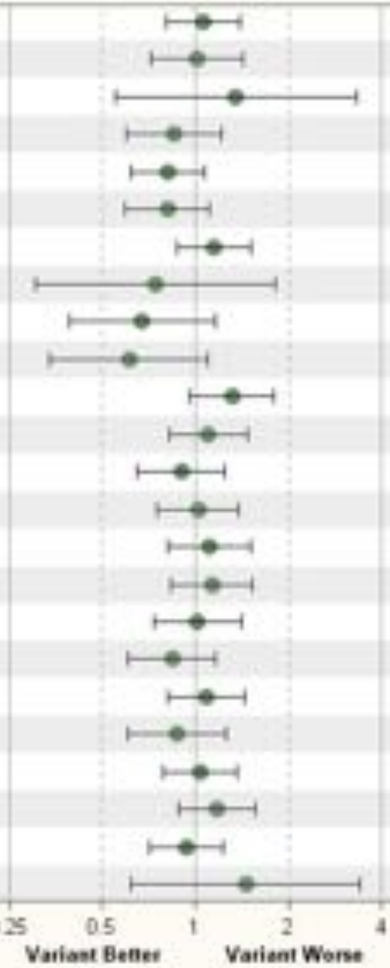

Adenosine Inhibits Matrix Metalloproteinase-9 Secretion By Neutrophils

Implication of A2a Receptor and cAMP/PKA/Ca^{2+} Pathway

Isabelle Ernens, Didier Rouy, Emilie Velot, Yvan Devaux, Daniel R. Wagner

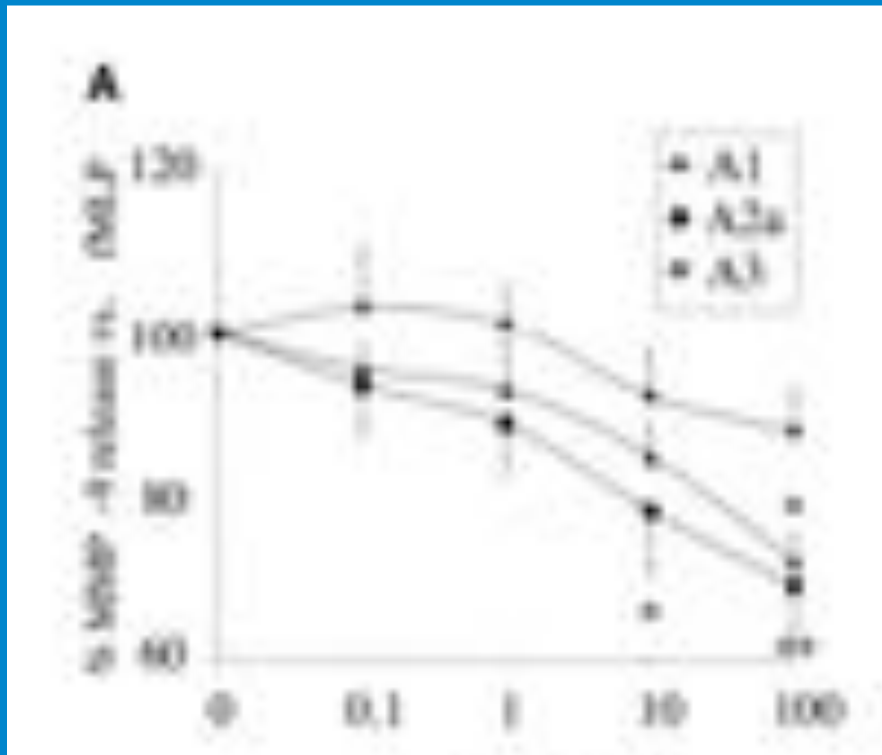

Circ Res, 2006

Rat LAD occlusion model of remodeling using micro PET

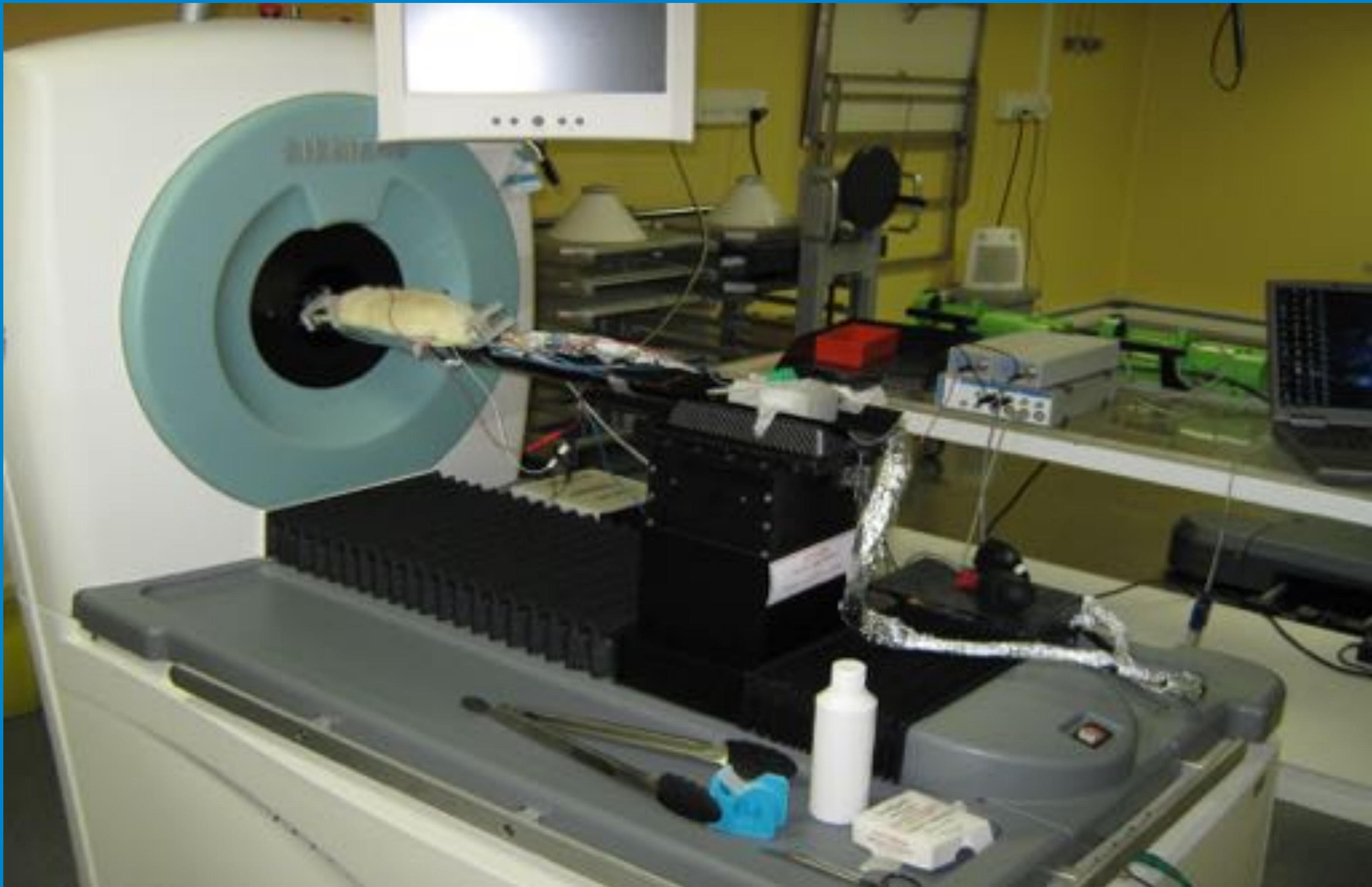

Cardioprotective effects of adenosine within the border and remote areas of myocardial infarction

Mélanie Bousquenaud[1], Fatiha Maskali[2], Sylvain Poussier[2], Jennifer Zangrando[1], Pierre Yves Marie[2,3], Henri Boutley[2], Renaud Fay[4], Gilles Karcher[2], Daniel R Wagner[1,5] and Yvan Devaux[1*]

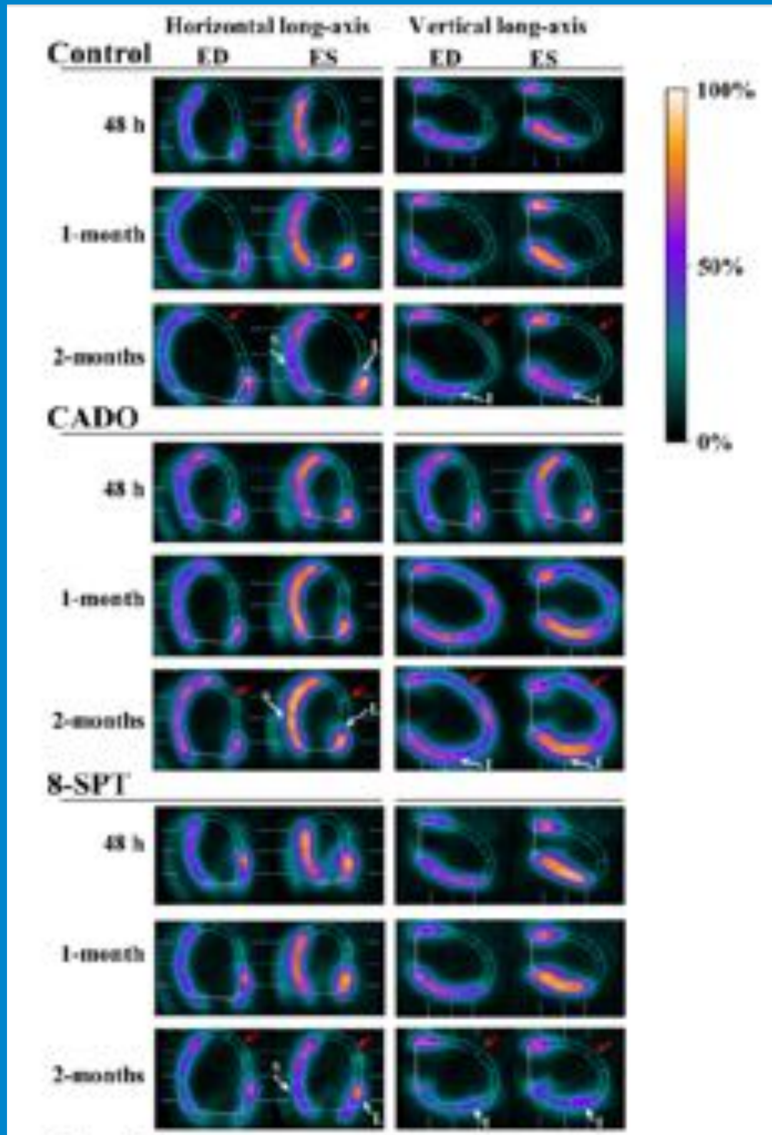

EJNMMI Res, 2013

Info-bio

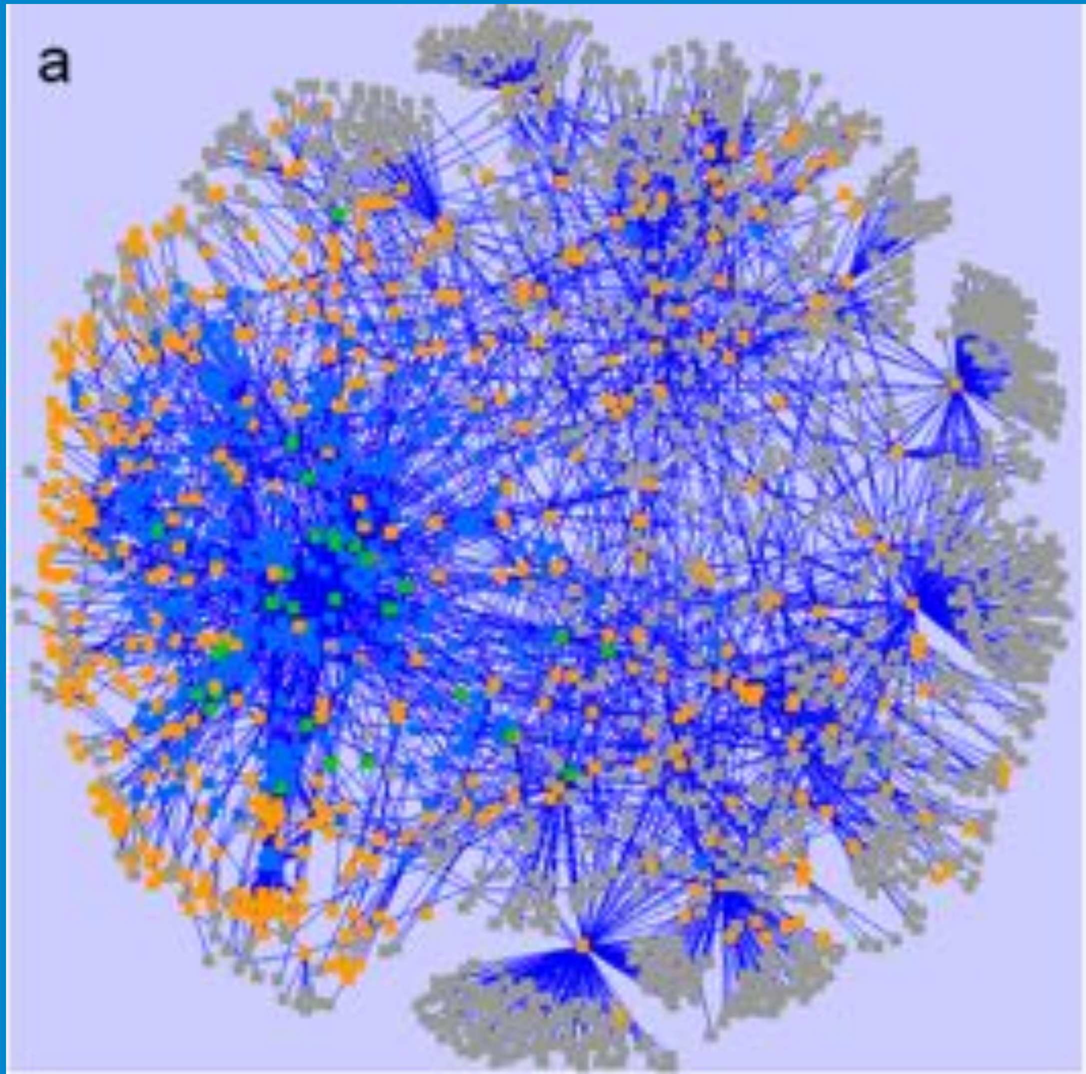

Azuaje et al., Nature Scientific Reports, 2011

RESEARCH ARTICLE Open Access

Coordinated modular functionality and prognostic potential of a heart failure biomarker-driven interaction network

Francisco Azuaje*[1], Yvan Devaux[1] and Daniel R Wagner[1,2]

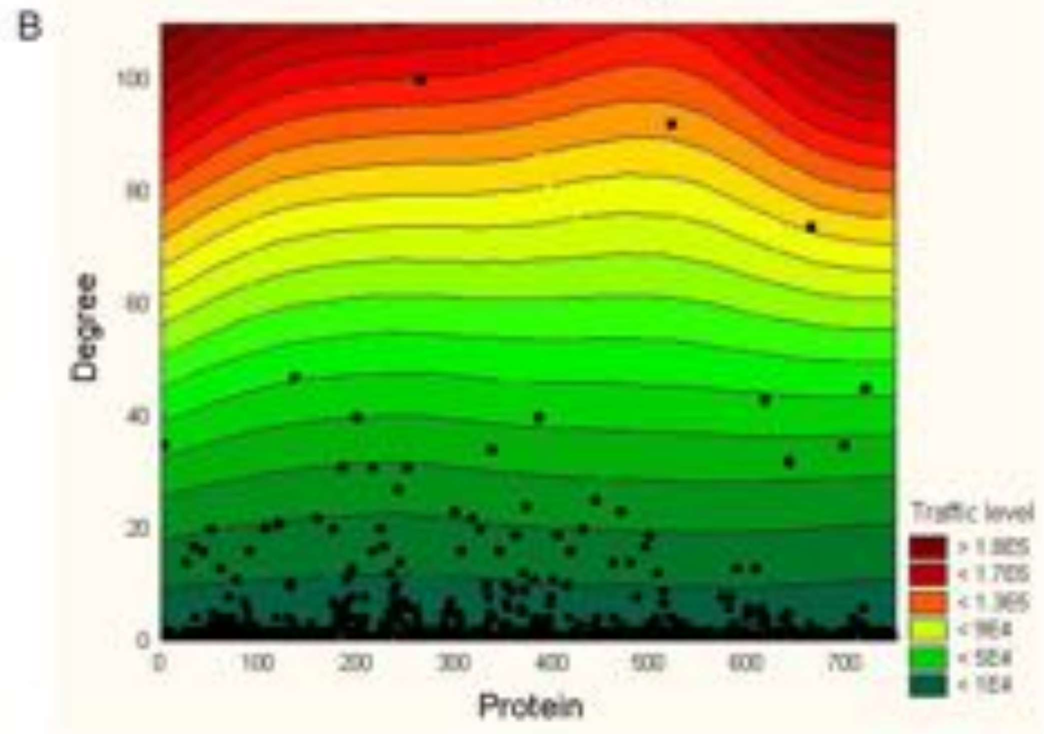

Figure 4 Characterization of major network communication properties. A. Relationship between node degree and traffic. B. A 3D contour plot of the communication and connectivity structure of the HF network. In A, a line is fitted to the data to highlight the linear relationship between the variables. In B, the black squares represent network proteins plotted against their corresponding degree values, and the colour-coded regions reflect the traffic levels. Colour regions and contours were fitted according to a distance-weighted least squares procedure. The higher the position of a protein on the plot, the larger its number of connections and traffic level. Fibronectin 1 (FN1), integrin beta 1 (ITGB1) and platelet-derived growth factor receptor beta (PDGFRB) are the top three communication "hotspots" with the highest degree and traffic values in this network.

BMC Systems Biology, 2010

Integrated protein network and microarray analysis to identify potential biomarkers after myocardial infarction

Yvan Devaux · Francisco Azuaje · Mélanie Vausort ·
Céline Yvorra · Daniel R. Wagner

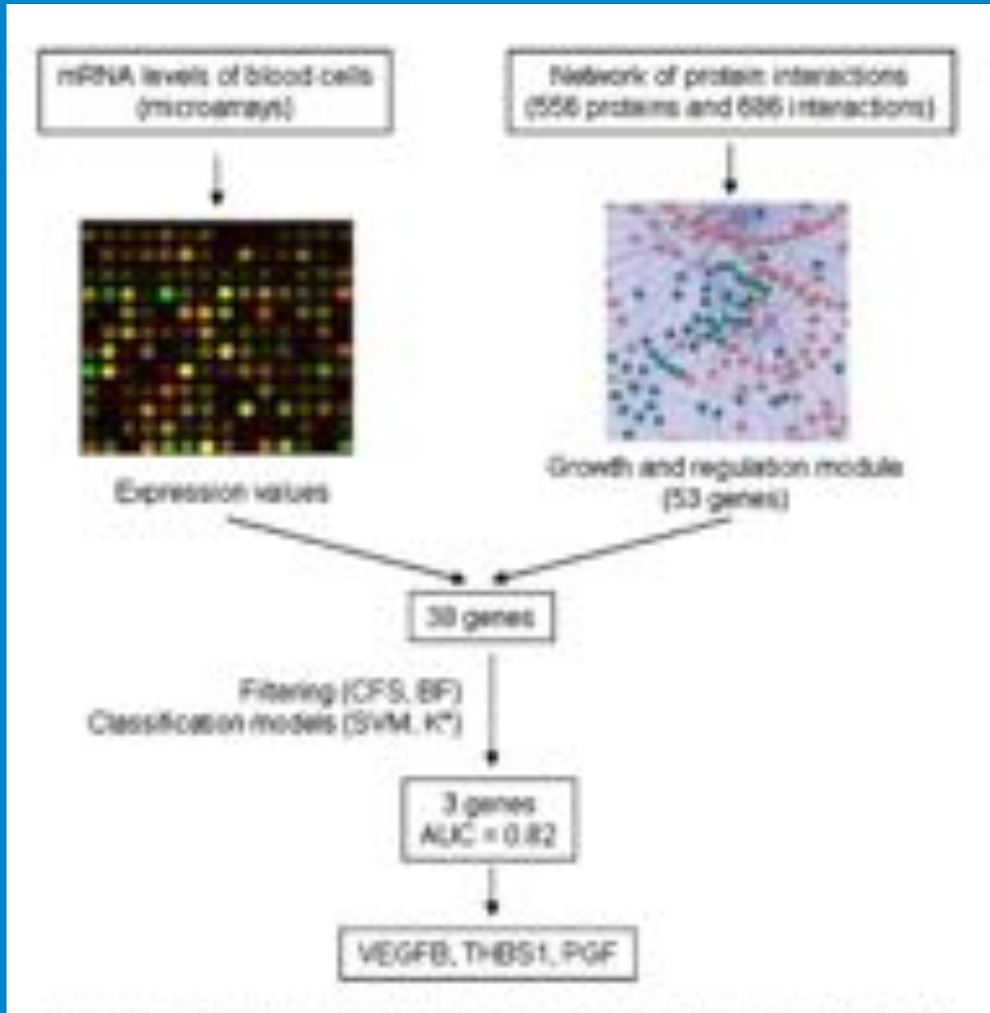

Funct Integr Genomics, 2010

Low Levels of Vascular Endothelial Growth Factor B Predict Left Ventricular Remodeling After Acute Myocardial Infarction

YVAN DEVAUX, PhD,[1] MELANIE VAUSORT, MSc,[1] FRANCISCO AZUAJE, PhD,[1] MICHEL VAILLANT, PhD,[2] MARIE-LISE LAIR,[3] ETIENNE GAYAT, MD, PhD,[4] JOHAN LASSUS, MD, PhD,[5] LEONG L. NG, MD,[6] DOMINIC KELLY, MD,[6] DANIEL R. WAGNER, MD, PhD,[1,7] AND IAIN B. SQUIRE, MD, PhD[6]

Luxembourg, Luxembourg; Leicester, United Kingdom; Paris, France; and Helsinki, Finland

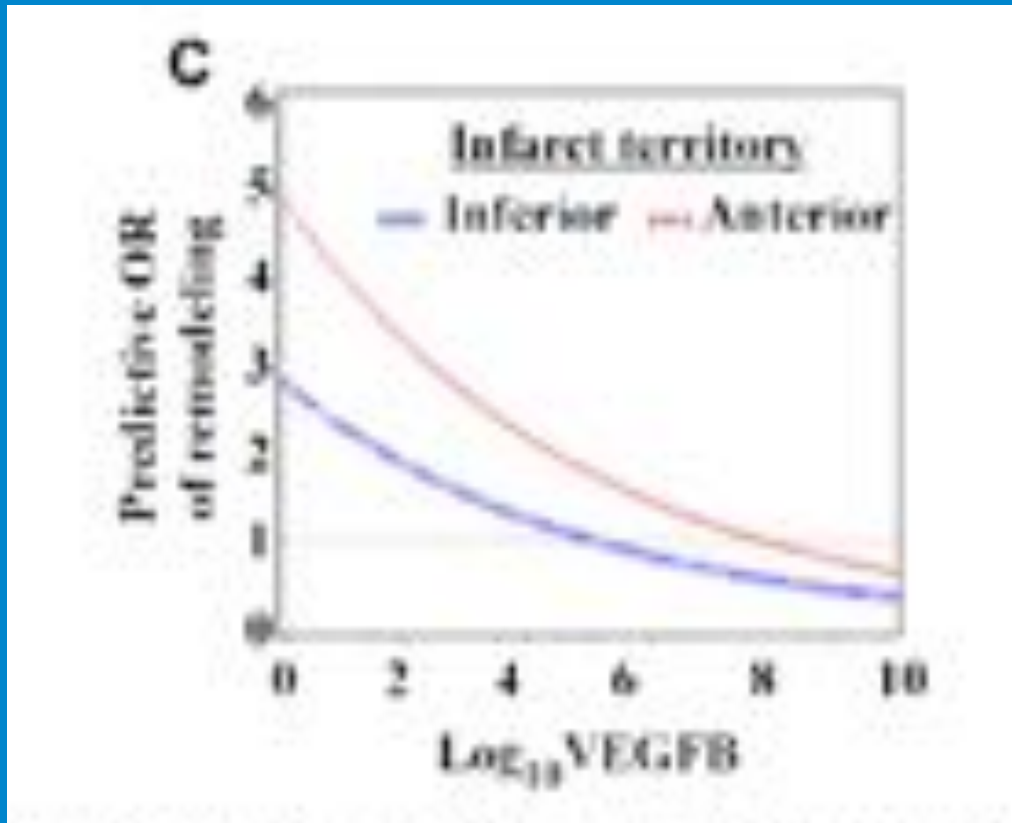

J Cardiac Failure, 2012

Non coding RNA

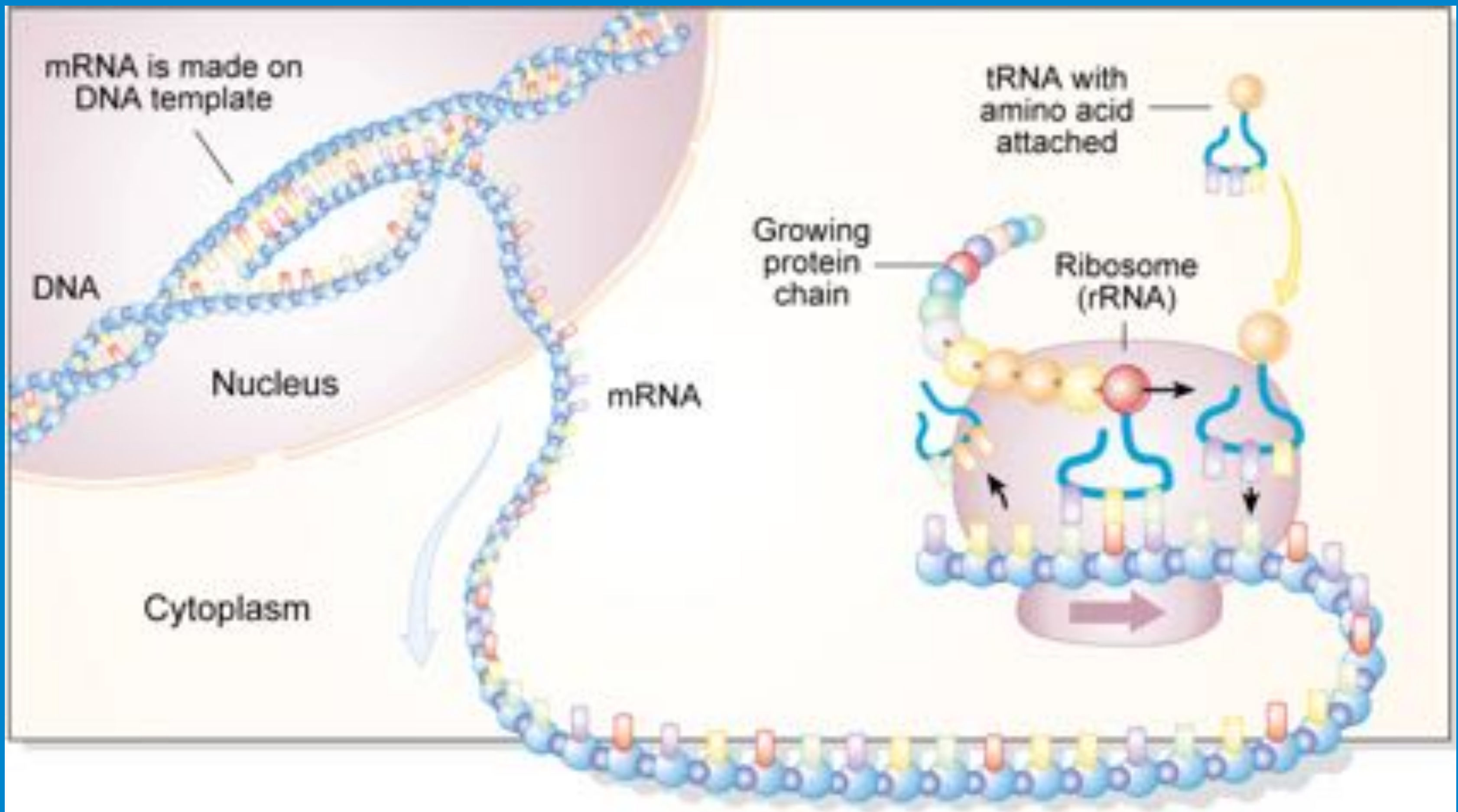

Circulating microRNAs after cardiac arrest*

Pascal Stammet, MD; Emeline Goretti, MSc; Mélanie Vausort, MSc; Lu Zhang, MSc; Daniel R. Wagner, MD, PhD; Yvan Devaux, PhD

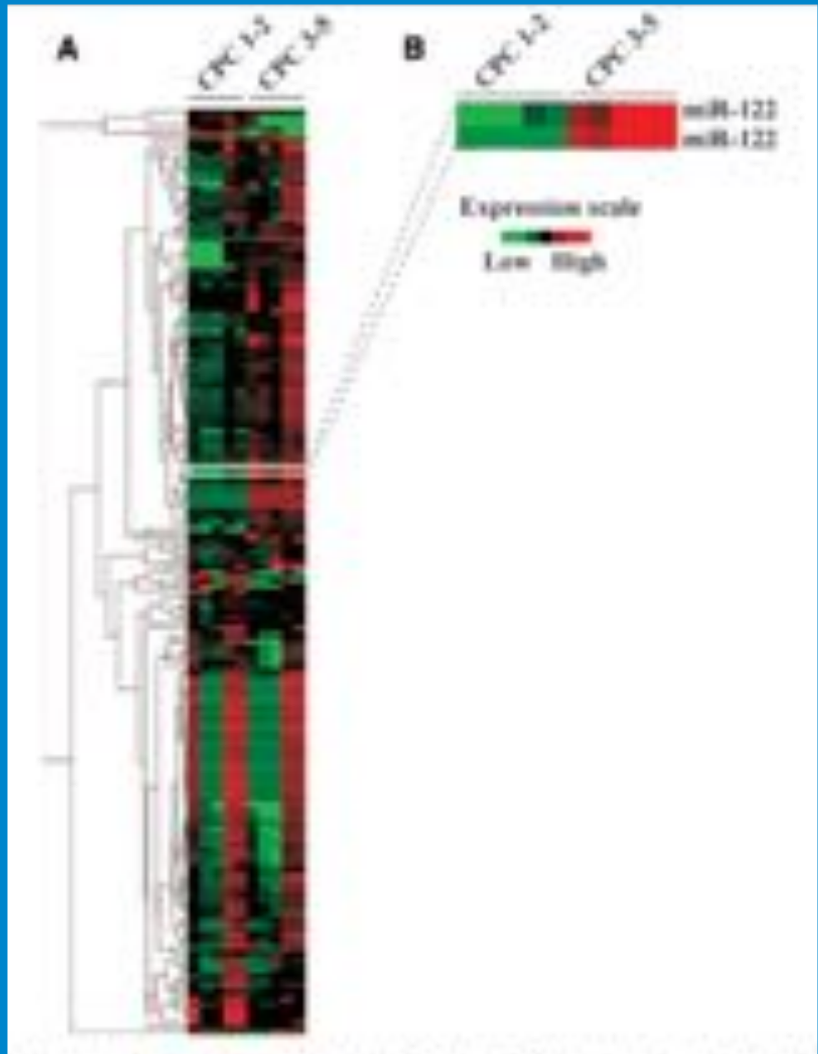

Critical Care Med, 2012

MicroRNA-150

A Novel Marker of Left Ventricular Remodeling After Acute Myocardial Infarction

Yvan Devaux, PhD; Melanie Vausort, MSc; Gerry P. McCann, MD; Jennifer Zangrando, MSc;
Dominic Kelly, MD; Naveed Razvi, MBBS; Lu Zhang, MSc; Leong L. Ng, MD;
Daniel R. Wagner, MD, PhD; Iain B. Squire, MD

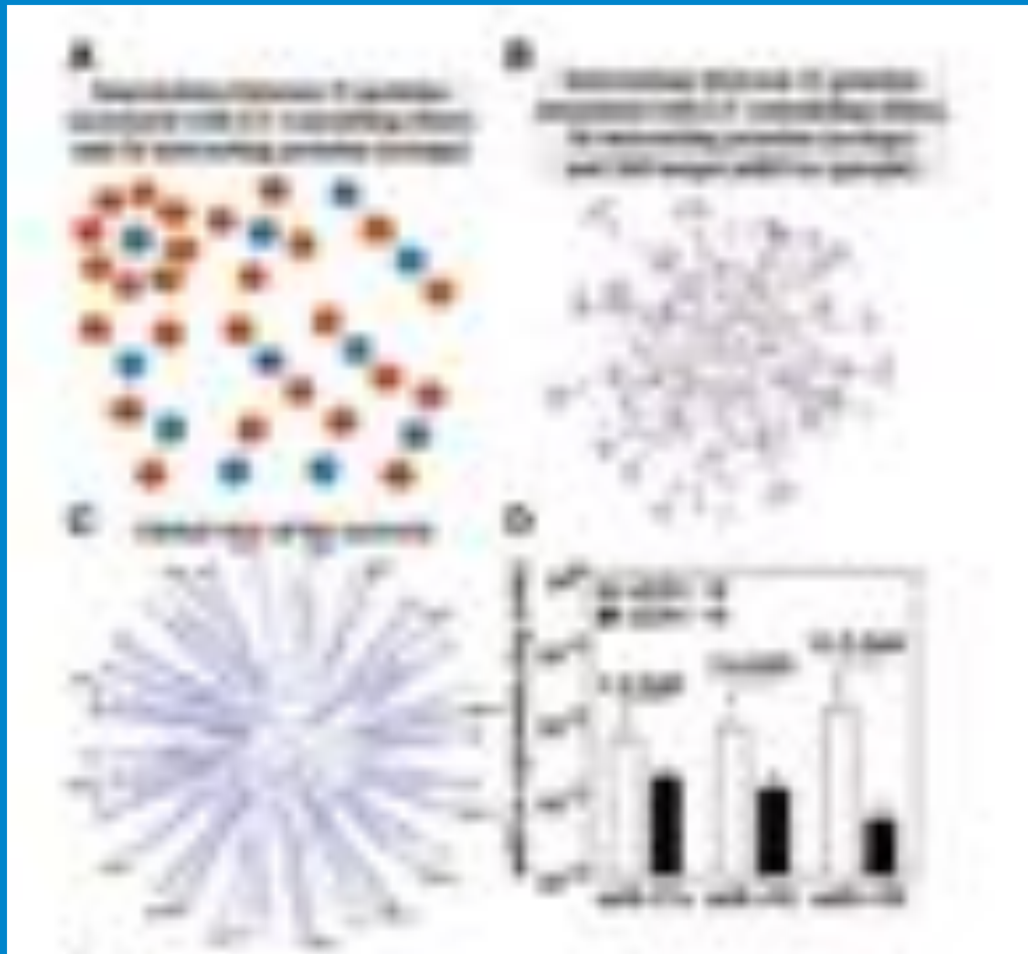

Circulation CV Genetics, 2013

Clinical Track

Long Noncoding RNAs in Patients With Acute Myocardial Infarction

Mélanie Vausort, Daniel R. Wagner, Yvan Devaux

Rationale: Long noncoding RNAs (lncRNAs) constitute a novel class of noncoding RNAs that regulate gene expression. Although recent data suggest that lncRNAs may be associated with cardiac disease, little is known about lncRNAs in the setting of myocardial ischemia.

Objective: To measure lncRNAs in patients with myocardial infarction (MI).

Methods and Results: We enrolled 414 patients with acute MI treated by primary percutaneous coronary intervention. Blood samples were harvested at the time of reperfusion. Expression levels of 5 lncRNAs were measured in peripheral blood cells by quantitative polymerase chain reaction: hypoxia inducible factor 1A antisense RNA 2, cyclin-dependent kinase inhibitor 2B antisense RNA 1 (ANRIL), potassium voltage-gated channel, KQT-like subfamily, member 1 opposite strand/antisense transcript 1 (KCNQ1OT1), myocardial infarction-associated transcript, and metastasis-associated lung adenocarcinoma transcript 1. Levels of hypoxia inducible factor 1A antisense RNA 2, KCNQ1OT1, and metastasis-associated lung adenocarcinoma transcript 1 were higher in patients with MI than in healthy volunteers (P<0.05), and levels of ANRIL were lower in patients with MI (P=0.003). Patients with ST-segment–elevation MI had lower levels of ANRIL (P<0.001), KCNQ1OT1 (P<0.001), myocardial infarction-associated transcript (P<0.001), and metastasis-associated lung adenocarcinoma transcript 1 (P=0.005) when compared with patients with non-ST-segment–elevation MI. Levels of ANRIL were associated with age, diabetes mellitus, and hypertension. Patients presenting within 3 hours of chest pain onset had elevated levels of hypoxia inducible factor 1A antisense RNA 2 when compared with patients presenting later on. ANRIL, KCNQ1OT1, myocardial infarction-associated transcript, and metastasis-associated lung adenocarcinoma transcript 1 were significant univariable predictors of left ventricular dysfunction as assessed by an ejection fraction ≤40% at 4-month follow-up. In multivariable and reclassification analyses, ANRIL and KCNQ1OT1 improved the prediction of left ventricular dysfunction by a model, including demographic features, clinical parameters, and cardiac biomarkers.

Conclusions: Levels of lncRNAs in blood cells are regulated after MI and may help in prediction of outcome. This motivates further investigation of the role of lncRNAs after MI. (*Circ Res.* 2014;115:668-677.)

Matrix Metalloproteinase-9 (MMP-9)	-
Vascular Endothelial Growth Factor-B (VEGFB)	+
Thrombospondin-1 (THB-1)	-
Placental Growth Factor (PGF)	-
Micro-RNA-150	+
Micro-RNA-101	+
Micro-RNA-27a	-
Micro-RNA-16	-

Heart Regeneration in Zebrafish

Kenneth D. Poss,* Lindsay G. Wilson, Mark T. Keating*

Cardiac injury in mammals and amphibians typically leads to scarring, with minimal regeneration of heart muscle. Here, we demonstrate histologically that zebrafish fully regenerate hearts within 2 months of 20% ventricular resection. Regeneration occurs through robust proliferation of cardiomyocytes localized at the leading epicardial edge of the new myocardium. The hearts of zebrafish with mutations in the Mps1 mitotic checkpoint kinase, a critical cell cycle regulator, failed to regenerate and formed scars. Thus, injury-induced cardiomyocyte proliferation in zebrafish can overcome scar formation, allowing cardiac muscle regeneration. These findings indicate that zebrafish will be a useful for genetically dissecting the molecular mechanisms of cardiac regeneration.

Injured human hearts do not regenerate. Instead, damaged myocardium is replaced by fibrotic scar tissue. Cardiomyocytes, the major structural cells of the heart, may undergo hypertrophy in the wound area to increase muscular mass. Although recent findings suggest that cardiomyocytes within the damaged human heart can proliferate (1), most evidence to date indicates that myocyte proliferation is not a significant component of the mammalian response to cardiac injury (2).

Teleost fish, including zebrafish, can regenerate spinal cord, retina, and fins (3, 4). To determine whether zebrafish can also regenerate heart muscle, we surgically removed ~20% of the ventricular myocardium from 1- to 2-year-old adults (Fig. 1, A and B) and

Department of Cell Biology, Department of Cardiology, Howard Hughes Medical Institute, Harvard Medical School, Children's Hospital, 320 Longwood Avenue, Boston, MA 02115, USA.

*To whom correspondence should be addressed. E-mail: kposs@enders.tch.harvard.edu (K.D.P.); mkeating@enders.tch.harvard.edu (M.T.K.)

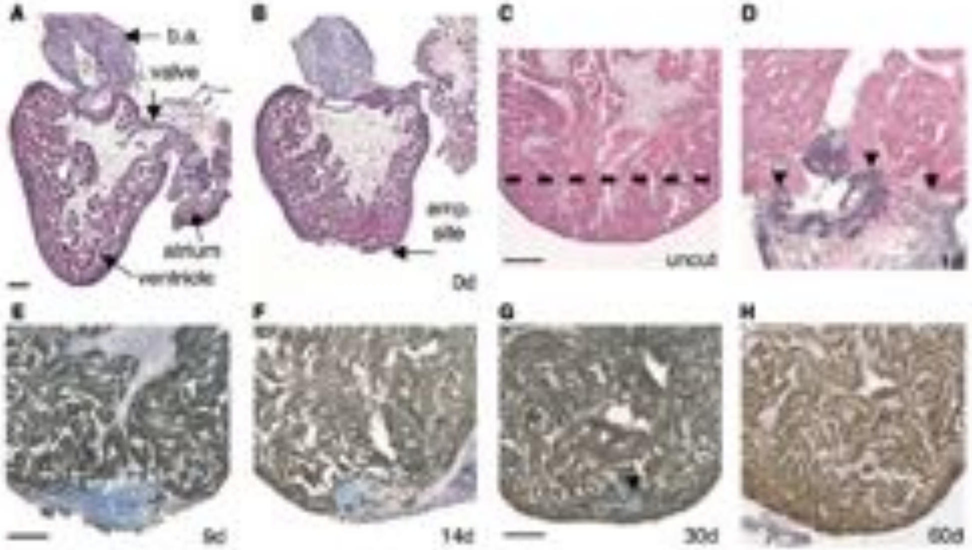

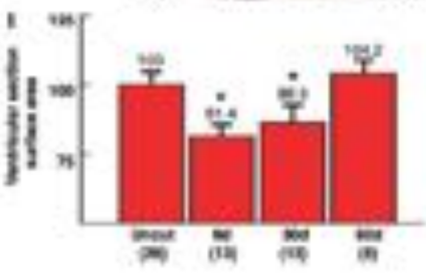

Fig. 1. Regeneration of ventricular myocardium in the resected zebrafish heart. Hematoxylin and eosin stain of the intact zebrafish heart before (A) and after about 20% ventricular resection (B) (5). b.a., bulbous arteriosus. (C) An intact ventricular apex at higher magnification, indicating the approximate amputation plane (dashed line). All images in this and subsequent figures display longitudinal ventricular sections of the amputation plane. (D) 1 dpa. The large clot is filled with nucleated erythrocytes (arrowheads). (E) 9 dpa. The heart section is stained for the presence of myosin heavy chain to identify cardiac muscle (brown) and with aniline blue to identify fibrin (blue) (5). The apex is sealed with a large amount of mature fibrin. (F) 14 dpa. The fibrin has diminished, and the heart muscle has reconstituted. (G) 30 dpa. A new cardiac wall has been created, and only a small amount of internal fibrin remains (arrowhead). (H) 60 dpa. This ventricle shows no sign of injury. (I) Quantification of healing at 0, 30, and 60 dpa. Values represent the size of the largest ventricular section (mean ± SEM, *P < 0.05); parentheses indicate the number of hearts examined (5). Scale bars, 100 μm.

Anatomy of zebrafish heart

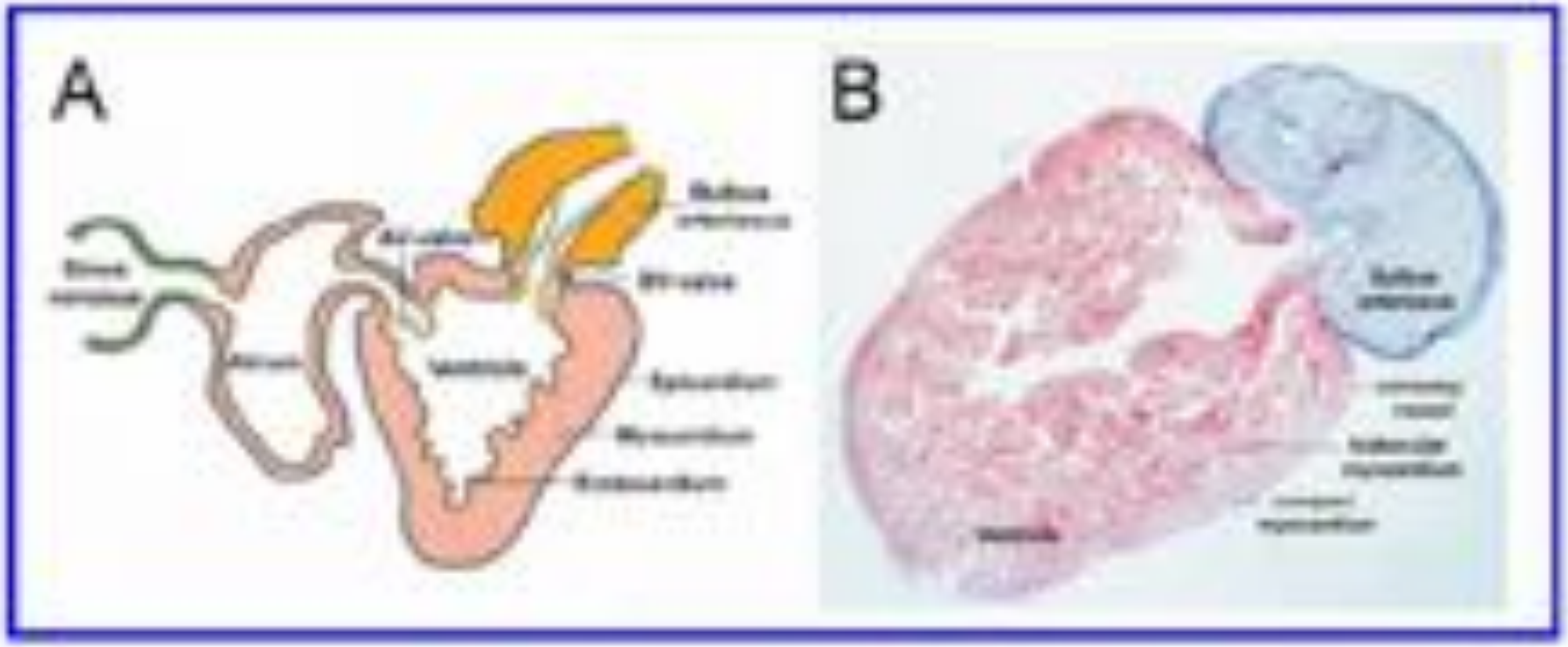

Swim tunnel

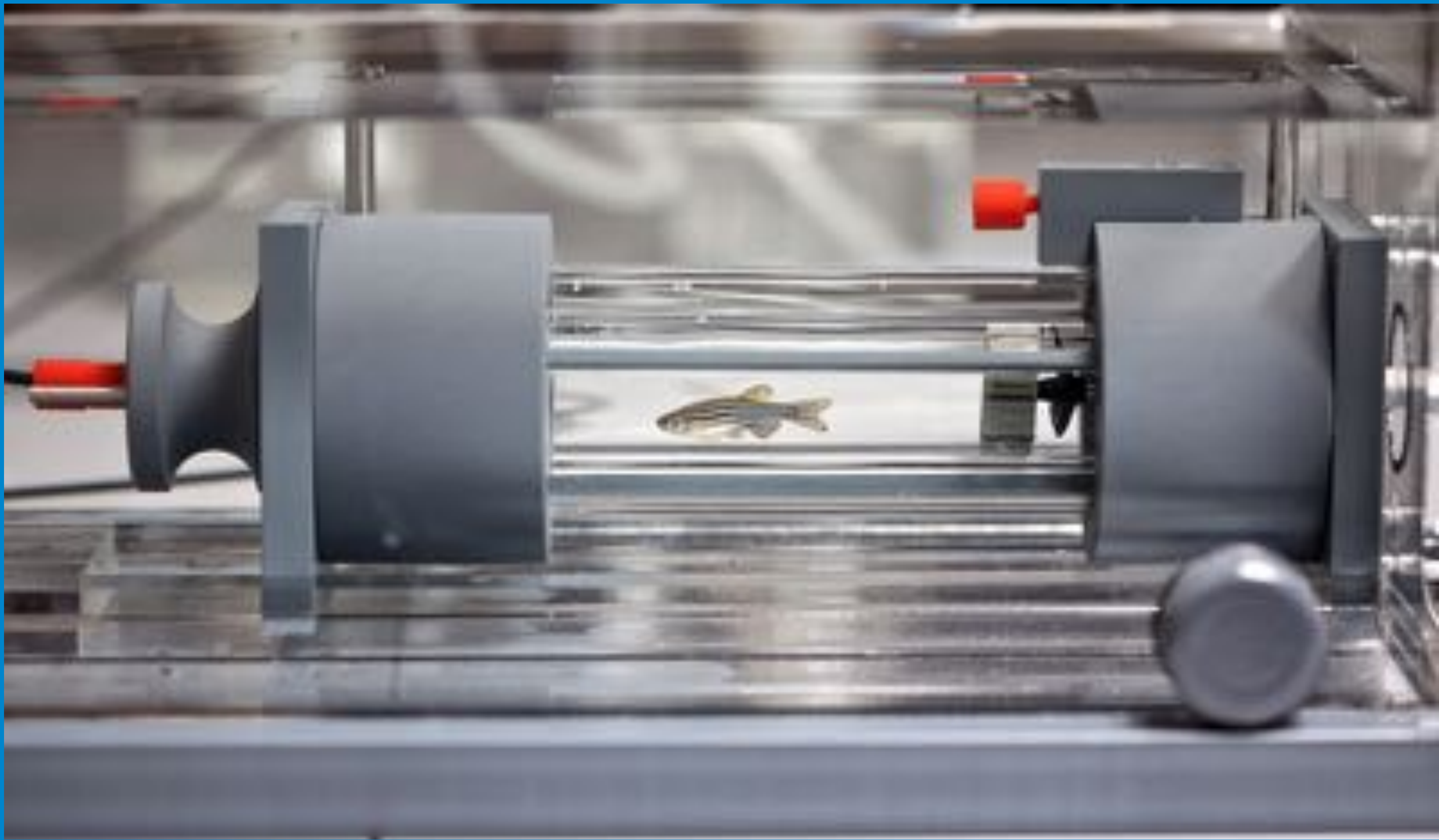

OCT

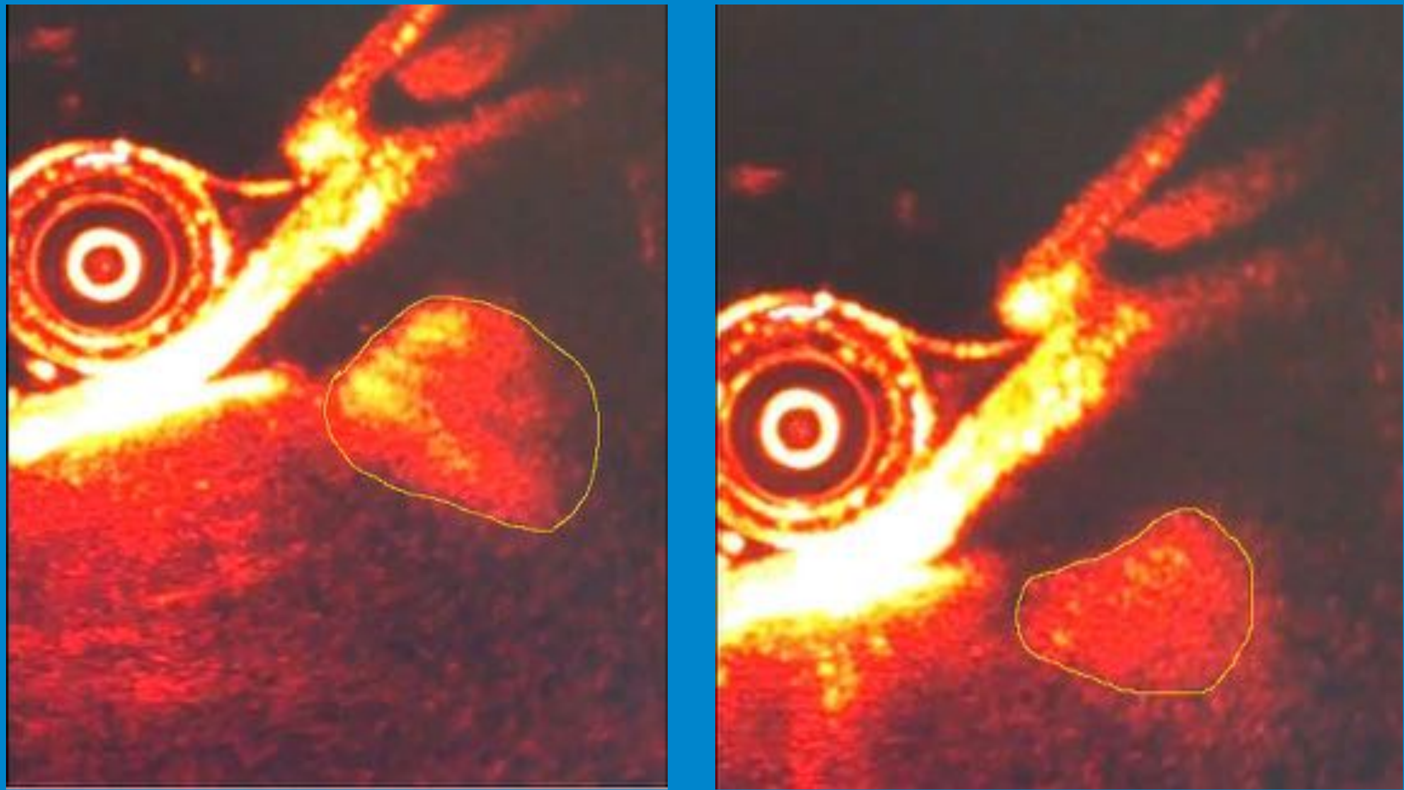

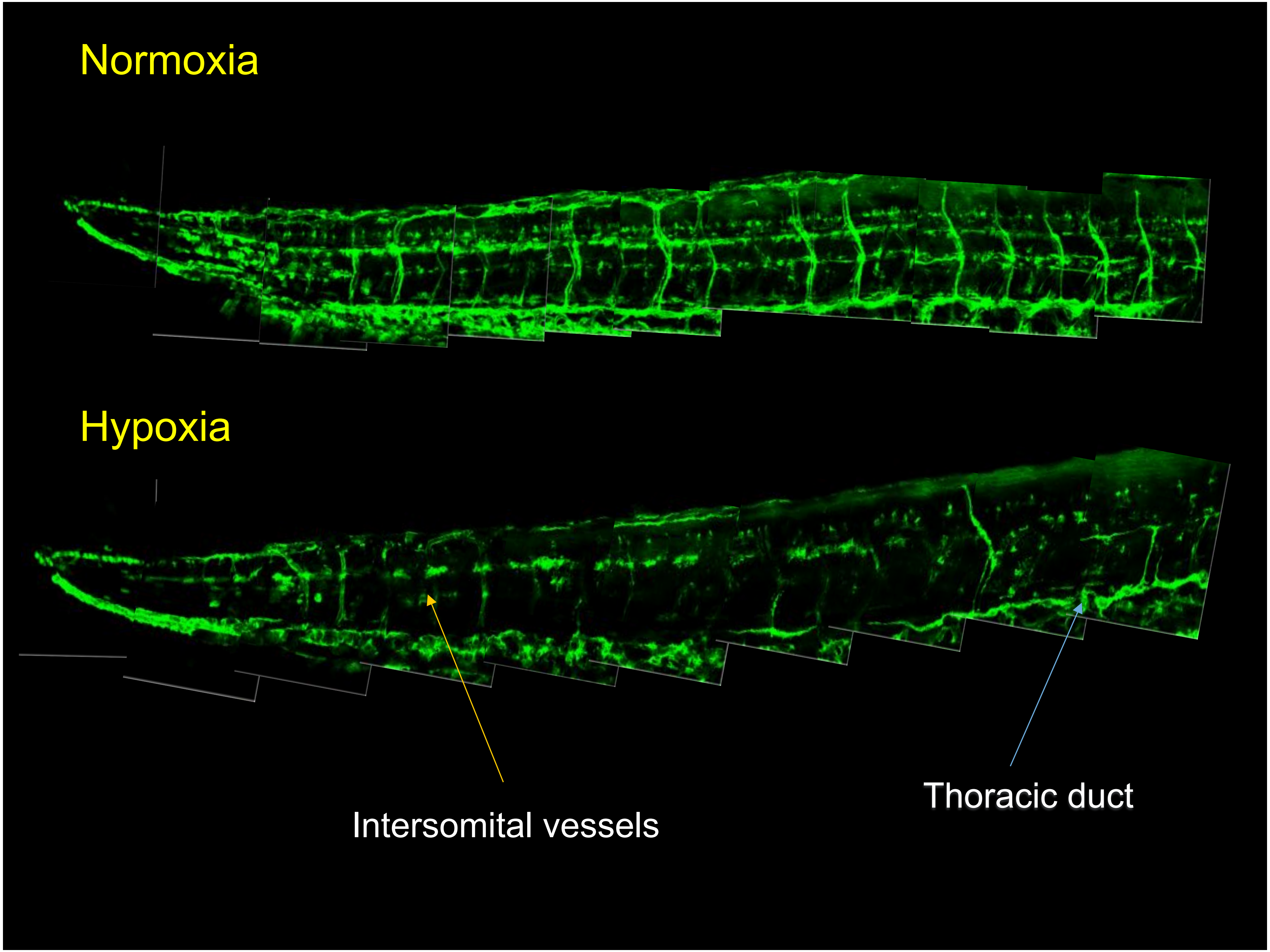
Normoxia
Hypoxia
Intersomital vessels
Thoracic duct

Zebrafish with heart failure

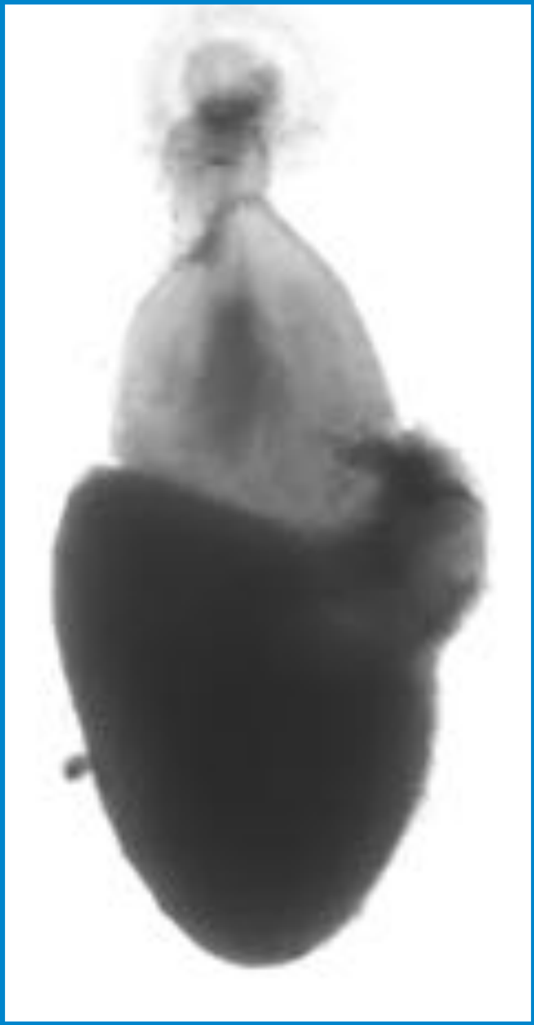

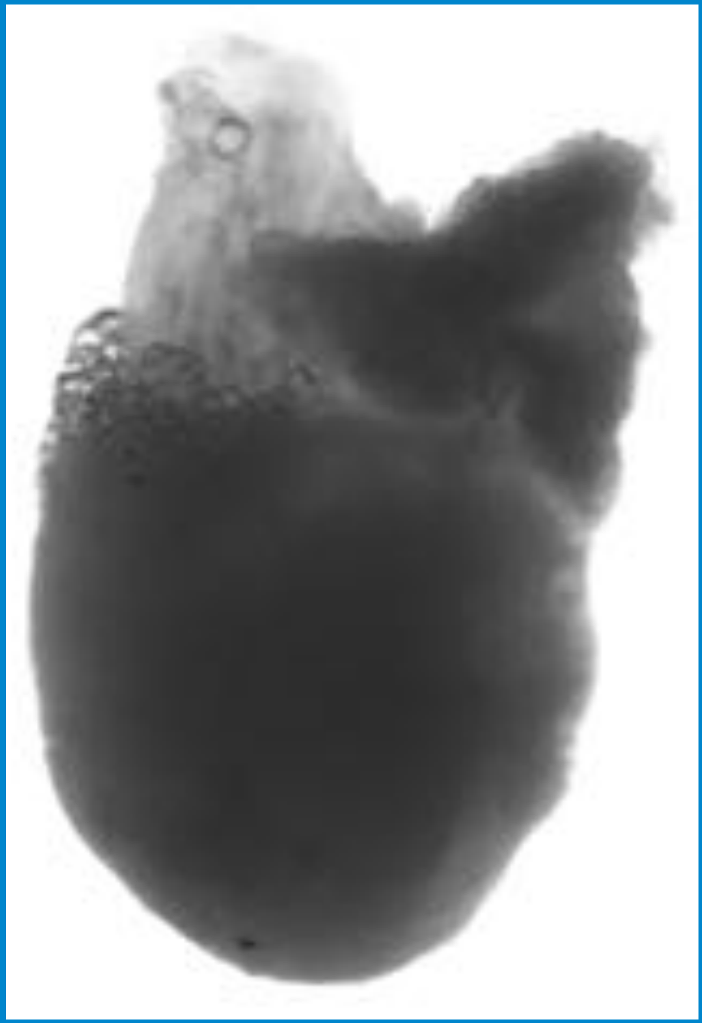

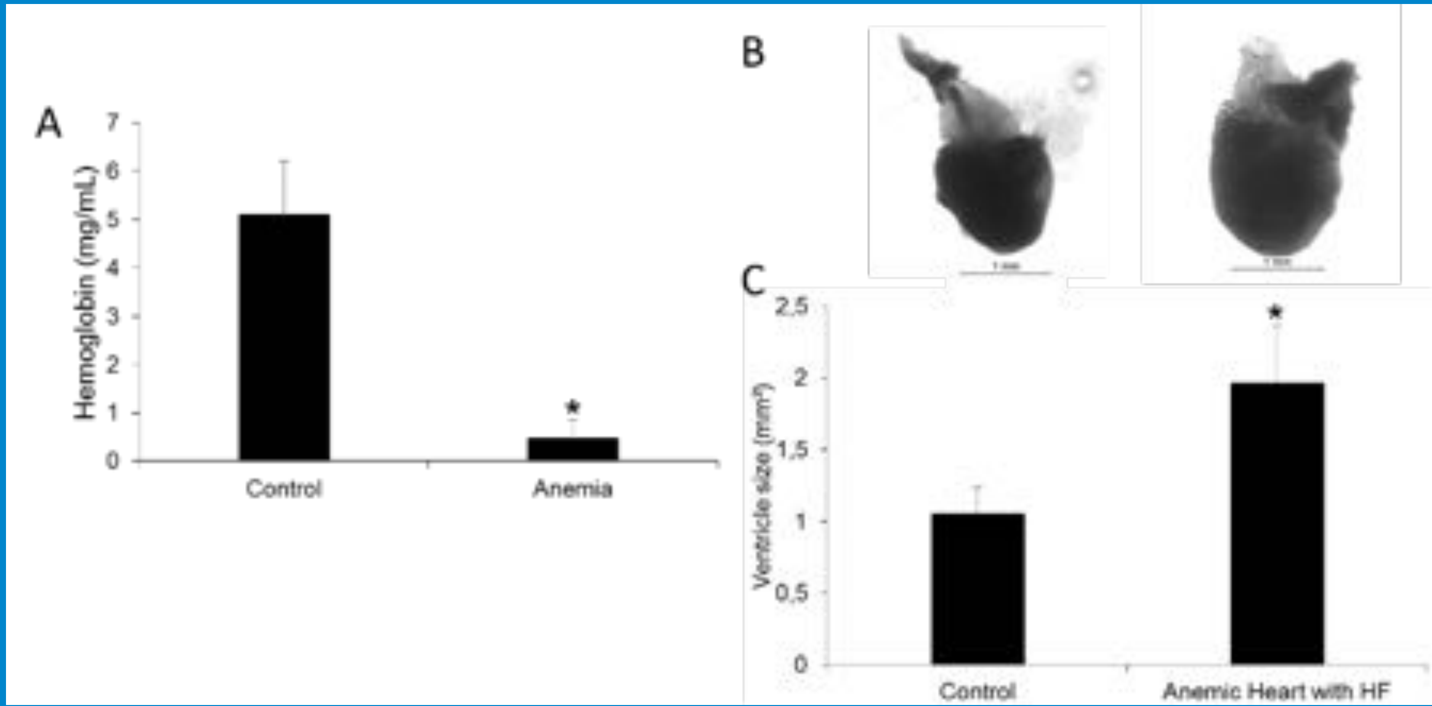
A
Hemoglobin (mg/mL)
0
1
2
3
4
5
6
7
*
Control
Anemia
B
C
Ventricle size (mm²)
0
0,5
1
1,5
2
2,5
*
Control
Anemic Heart with HF

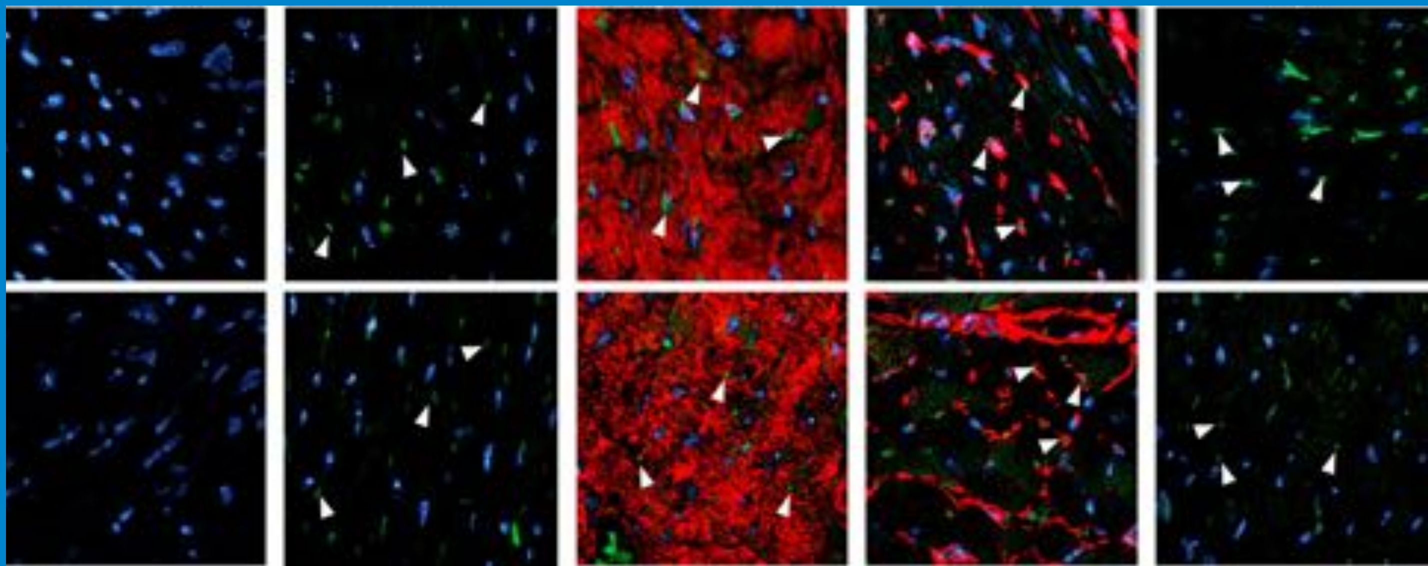

Zebrafish with diabetes

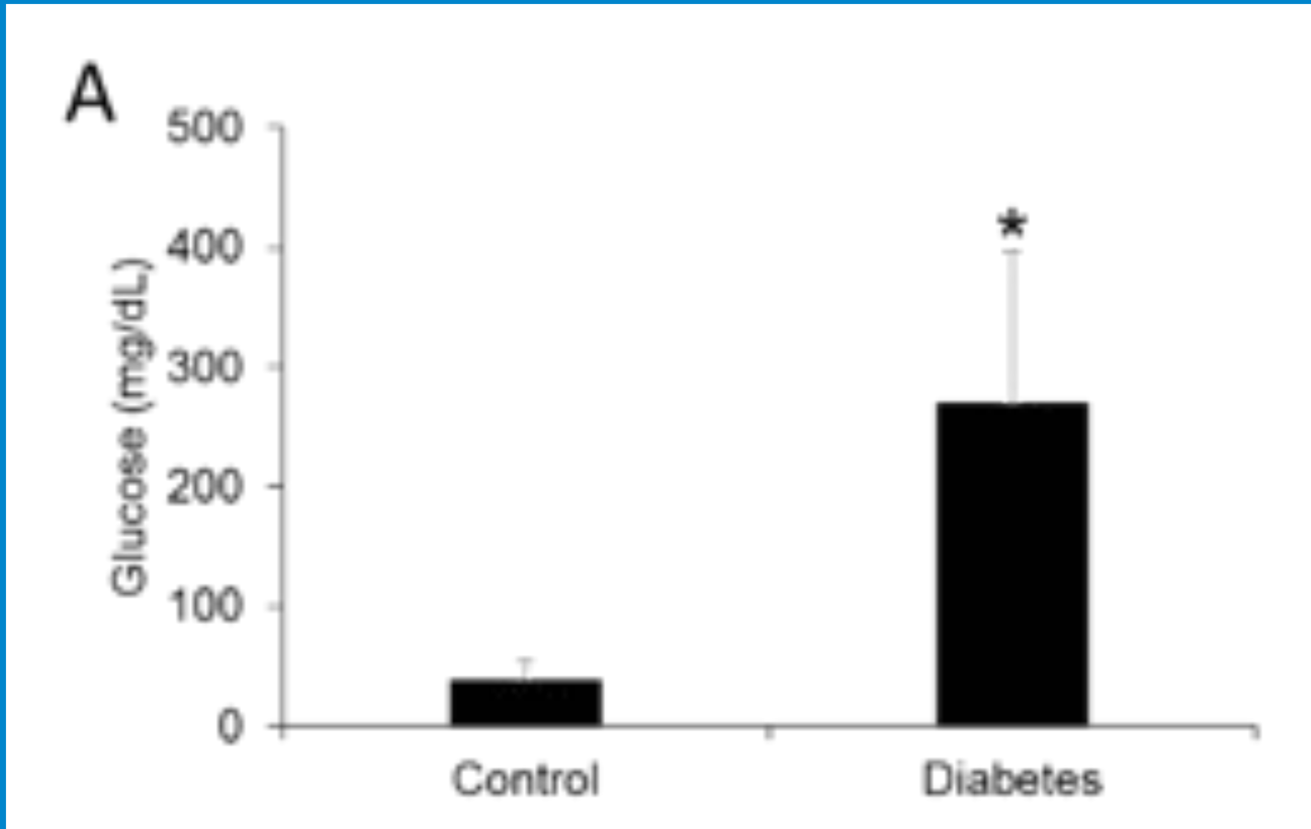

Conclusions

- Info-bio aide à mieux comprendre les effets de l'infarctus et à trouver de nouveaux biomarqueurs
- Le poisson-zèbre est idéal pour étudier les mécanismes moléculaires et de nouveaux traitements
- Une prise en charge à la carte du patient avec infarctus devrait être possible dans le futur

I ♥

ZEBRAFISH